Title

Acute shear stress direction dictates adherent cell remodeling and verifies shear profile of spinning disk assays

Journal

Physical Biology, 12(1)

ISSN

1478-3967

Authors

Fuhrmann, Alexander
Engler, Adam J

Publication Date

2015

DOI

10.1088/1478-3975/12/1/016011

Peer reviewed

Acute shear stress direction dictates adherent cell remodeling and verifies shear profile of spinning disk assays

2015 Phys. Biol. 12 016011

(http://iopscience.iop.org/1478-3975/12/1/016011)

Physical Biology

RECEIVED
6 August 2014

ACCEPTED FOR PUBLICATION
18 December 2014

PUBLISHED
21 January 2015

PAPER

Acute shear stress direction dictates adherent cell remodeling and verifies shear profile of spinning disk assays

Alexander Fuhrmann[1,2] **and Adam J Engler**[1,2]

[1] Departments of Bioengineering, University of California, San Diego, La Jolla, CA 92093, USA
[2] Sanford Consortium for Regenerative Medicine, La Jolla, CA 92037, USA

E-mail: aengler@ucsd.edu

Keywords: cell adhesion, cytoskeleton, shear flow, cell–ecm interactions

Supplementary material for this article is available online

Abstract

Several methods have been developed to quantify population level changes in cell attachment strength given its large heterogeneity. One such method is the rotating disk chamber or 'spinning disk' in which a range of shear forces are applied to attached cells to quantify detachment force, i.e. attachment strength, which can be heterogeneous within cell populations. However, computing the exact force vectors that act upon cells is complicated by complex flow fields and variable cell morphologies. Recent observations suggest that cells may remodel their morphology and align during acute shear exposure, but contrary to intuition, shear is not orthogonal to the radial direction. Here we theoretically derive the magnitude and direction of applied shear and demonstrate that cells, under certain physiological conditions, align in this direction within minutes. Shear force magnitude is also experimentally verified which validates that for spread cells shear forces and not torque or drag dominate in this assay, and demonstrates that the applied force per cell area is largely independent of initial morphology. These findings suggest that direct quantified comparison of the effects of shear on a wide array of cell types and conditions can be made with confidence using this assay without the need for computational or numerical modeling.

Introduction

Integrin-mediated adhesion to extracellular matrix (ECM) plays a central role in transducing mechanical signals to and from the cell's immediate environment in a process called mechanotransduction [1]. Integrins respond to a variety of physical stimuli including hydrostatic pressure, stretching, osmotic forces, and fluid shear stress by converting these mechanical signals into biochemical signals [2]; it is these biochemical signals that then guide a variety of cell functions such as proliferation or differentiation [2, 3]. A complimentary role for integrins is to connect the cell's actin cytoskeleton via large supramolecular complexes called focal adhesions (FAs) to ECM to facilitate 'inside-out' and 'outside-in' force transmission [1]. Active cell contractions and FAs are essential for mechanosensing as cells 'feel' their substrate by dynamically pulling at it and using FAs as another source of mechanotransductive signaling. Adhesions also must be dynamic; during migration for example cells need to form and mature at the leading edge while disassembling them at the trailing edge [4]. While the size and number of integrins often correlate with the overall adhesion strength, the complex interplay within cells and variability between cells makes predictions of attachment strength unreliable [5]. Since adhesion is ubiquitous to all adherent cells and is involved in many critical processes, e.g. cancer cell migration [6], quantitative information of cell adhesion strength is fundamental for understanding cell–ECM interactions.

To quantify differences in adhesion between cells, several techniques have been developed including cell force spectroscopy, micropipette aspiration, centrifugation, and shear stress assays [7, 8]. These assays all apply forces during short periods of time often over a limited area to quantify attachment strength, which minimizes cellular responses like bond strengthening due to these forces [9]. Under acute, high shear stress,

cell detachment is often assumed to occur as a unit in which all adhesions (including integrins) are stressed somewhat equally [10]. Recent data however indicates that cells can remodel their morphology and detach by a gradual peeling mechanism even during acute shear exposure [5]. Under certain physiologically-relevant cation concentrations cells subjected to acute shear can remodel their morphology by more than doubling their aspect ratio and aligning within minutes upon application of acute shear [5] as they do with longer-term exposure to shear [11]. While (dynamic) mechanisms guiding cellular remodeling are unclear, it does affect the cells' ability to withstand shear and thus the measured attachment strength, warranting a closer look at cell detachment under shear.

One device that quantifies the detachment forces of a cell population via acute shear exposure is the radial shear assay, i.e. spinning disk, which uses a rotating rod submerged in spinning buffer [10]. Cells adhering to coverslips mounted on the rod are then subjected to shear, which is correlated with radial distance. This enables high reproducibility and throughput over a wide range of shear within a single sample. However, as flow patterns have yet to be verified from their analytical solutions, both the magnitude and direction of the stresses acting on cells are difficult to quantify [8, 10]. Furthermore, the actual force on the cells depends on their morphology, which can vary between cells, thus complicating inter-cell comparisons. Here we experimentally verify the predicted shear profile applied on the cells with this assay in two steps: first upon systematic variation of the variables, we verify that the viscosity, radial position and rotational speed are correctly described in the shear force equation associated with the radial shear assay. Second, we verify the direction of flow by subjecting cells to shear conditions promoting cellular alignment as previously described [5]. Here we improve the alignment efficiency significantly, enabling us to precisely determine the alignment direction, which is not tangential to the disk rotation as one might expect. As alignment direction agrees well with the theoretically predicted flow direction this completes verification of the shear flow in spinning disk devices and also further demonstrates that cells can remodel their morphology to align with the direction of applied shear. Lastly, this allows us to estimate the forces that act on cells; for spread cells, typical variations in cell morphology result only in small, negligible variations in normalized force (force per cell spread area). Together, these data strengthen the suitability of such quantifiable shear force assays in measuring cell attachment strength but also highlight the importance of dynamic cellular responses during application of acute shear.

Materials and methods

Cell culture

Mouse NIH 3T3 fibroblast cells and human HT1080 fibrosarcoma cells were obtained from ATCC and cultured in DMEM with 10% bovine calf serum (3T3) or 10% fetal bovine serum (HT1080). All cells were cultured at 37 °C in a humidified incubator containing 5% carbon dioxide.

Spinning disk shear assay

25 mm glass coverslips (Fisher Scientific, St. Louis, MO) were sonicated with ethanol and deionized water before incubation of 10 μg ml^{-1} human fibronectin for 60 min at room temperature. 50 000 cells per coverslip were allowed to attach for several hours (as indicated) in media with or without serum (i.e. DMEM only) resulting in cell densities around 10 000 cells/cm^2. Coverslips were then mounted on a custom built spinning disk device and dipped into temperature controlled spinning buffer (37 °C). HEPES with 0.5 mM $MgCl_2$ and with or without 0.9 mM $CaCl_2$ (Cellgro, Manassas, VA) supplemented KCl and NaCl was used for the spinning buffer. Glycerol was used to increase the viscosity of the spinning buffer seven-fold by mixing 512 ml Glycerol to 488 ml HEPES to a 51% v/v solution [12]. Salts and ions were adjusted to keep their concentration constant based on previous measurements. However at the glycerol concentrations required to significantly increase the viscosity, 3T3 cells showed significant changes in morphology (pores) and detached under lower shear. Human fibrosarcoma cells were not glycerol sensitive, and thus they were used in spinning assays with glycerol and appropriate controls. All spinning buffers contained 4.5 mg ml^{-1} dextrose. Once immersed into the spinning buffer, coverslips were spun for 5 min (with exception of figure 6 where shear was applied for 10 min) at defined angular velocities and fixed with 3.7% formaldehyde immediately after spinning.

Flow above spinning disk

The flow above a rotating disk has been discussed multiple times previously, several analytical and numerical solutions of laminar flow near a rotating disk exists from Karman [13], Schlichting [14], Cochran [15], and Sohrab [16], respectively. Therefore we only discuss this problem here briefly and refer to the above mentioned literature for further details. To obtain the fluid flow components, local axial, azimuthal (tangential), and radial velocities (v_z, v_θ, and v_r, respectively) along the corresponding coordinates z, θ, and r are made dimensionless in the form

$$F(\xi) = \frac{v_r}{r \cdot \omega}, \quad G(\xi)\frac{v_\theta}{r \cdot \omega}, \quad H(\xi)\frac{v_z}{\sqrt{\nu \cdot \omega}}$$

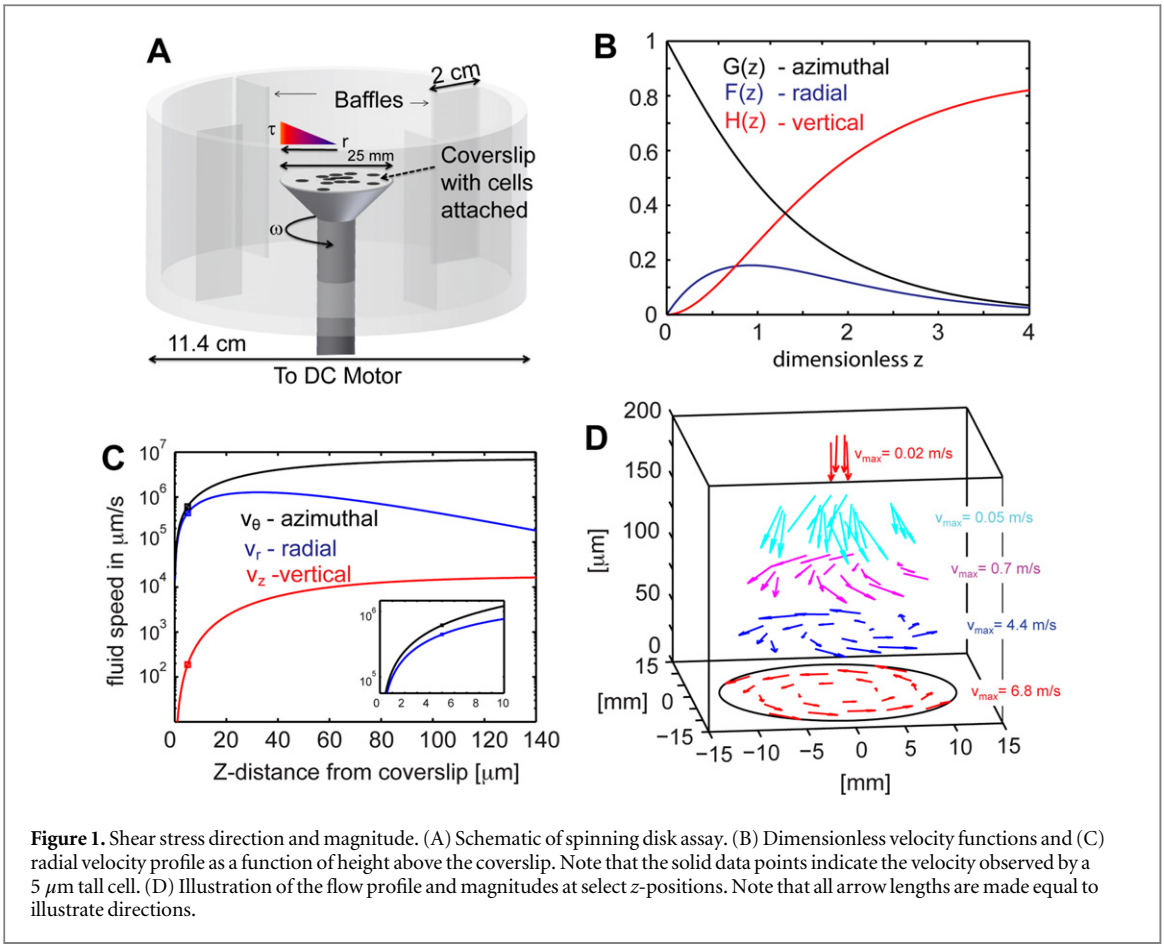

Figure 1. Shear stress direction and magnitude. (A) Schematic of spinning disk assay. (B) Dimensionless velocity functions and (C) radial velocity profile as a function of height above the coverslip. Note that the solid data points indicate the velocity observed by a 5 μm tall cell. (D) Illustration of the flow profile and magnitudes at select z-positions. Note that all arrow lengths are made equal to illustrate directions.

with

$$\xi = z\sqrt{\frac{\omega}{\nu}},$$

where ω is the angular velocity of the disk, ν is the kinematic viscosity and H results from mass conservation. These dimensionless variables, when applied to the Navier–Stokes equations and integrated, provide values for F, G and H assuming no-slip conditions. The wall shear stress, i.e. shear force, for Newtonian fluids is defined as

$$\tau = \mu \left.\frac{\partial \mathrm{v}}{\partial z}\right|_{z=0},$$

where μ is the dynamic viscosity, v the fluid velocity, and z is the height above the wall. Shears stress is reported in dyne/cm^2, which is the commonly used unit in these assays. Note that 1 dyne/cm^2 is equal to 0.1 Pa.

Immunofluorescence

Fixed cells were incubated for 10 min with 0.25% Triton X-100 followed by 1% albumin over night at 4 °C for blocking. Rhodamine phalloidin (1:2000 Invitrogen) and Hoechst 33342 (3.2 μM, Invitrogen) were applied for 30 min at room temperature. Cells were subsequently mounted with Fluoromount-G (Southern Biotech, Birmingham, AL). All buffers used contained 1 mM MgCl2. Samples were imaged by a CARV II confocal (BD Biosciences) Nikon Eclipse Ti–S microscope equipped with a motorized, programmable stage using a Cool-Snap HQ camera (Photometrics) and controlled by Metamorph 7.6 (Molecular Devices). To obtain quantitative information of attachment strength and alignment, whole 25 mm coverslips were imaged at 10x magnification on a Nikon Ti–S microscope (~1000 individual images stitched together with Metamorph 7.6 software and custom macros) and analyzed using a custom written MATLAB program. Briefly, the user defines the outer circle of the coverslip from a stitched overview image and the software then finds the position of each nucleus relative to the center of the coverslip. Cell densities in dependence of radial position and subsequently shear, are stored and can be combined with other measurements at e.g. different rotations per minute (RPMs). A sigmoidal fit is used to quantify values of attachment strength and determine the statistical error of the fit. To obtain information of cell alignment, the actin cytoskeleton (Rhodamine phalloidin), is analyzed also using a custom written MATLAB program. Morphological parameters, i.e. length and orientation of major and minor axis from an ellipsoid fit, are determined and correlated to the position of the nucleus obtained previously. As the detection algorithm is fully automated, random

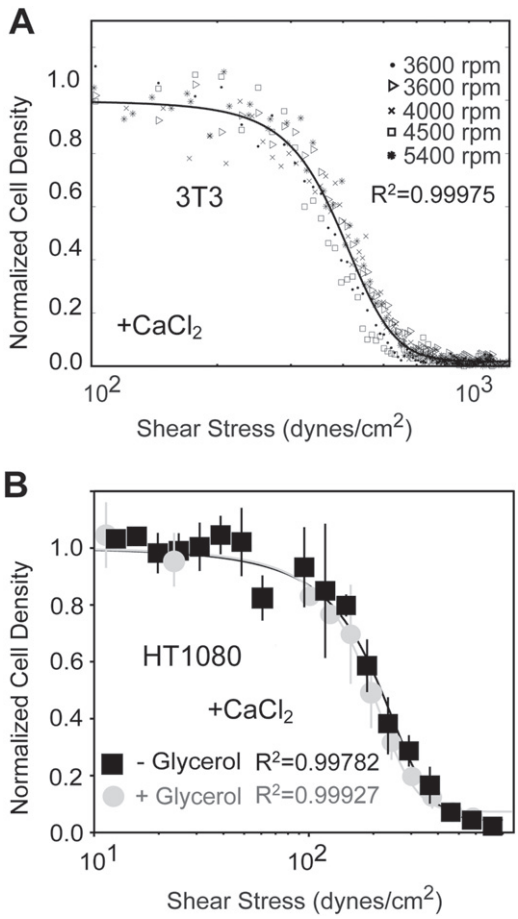

Figure 2. Cell density versus shear plots. Shear applied in presence of $CaCl_2$ (A) at multiple rotational speeds and (B) with and without a seven-fold change in viscosity via glycerol.

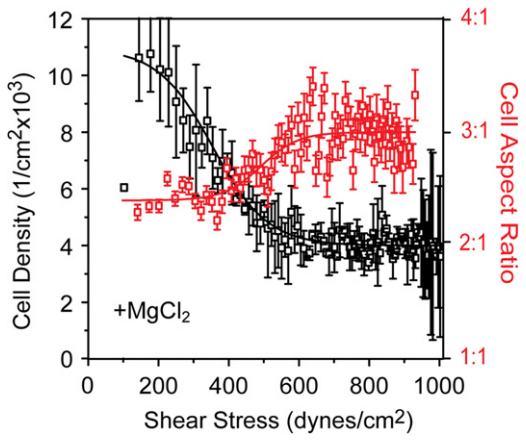

Figure 3. Plot of cell density (black) and aspect ratio (red) plotted against shear stress. Seeding cells without serum (24 h incubation) and spinning in $MgCl_2$ only containing buffer prevents complete cell detachment as ~40% of cells remain attached at higher shear (black). Also, average cell aspect ratio is increased in the remaining cells (red).

outliers will shift the measured cell alignment for symmetry reasons towards smaller values.

Statistics

All error bars represent the standard deviation from three or more biological replicates (i.e. separate measurements for which 4–6 coverslips where used each) except for the cell aspect ratio in figure 2(B) where error bars represent the error of the mean and data in figure 6(B) which were individual measurements. Averages of circular variables and further statistics were obtained with CircStat, a MATLAB toolbox for circular statistics [17].

Results and discussion

To determine if cell alignment is coordinated with shear direction and cell detachment is coordinated with shear force magnitude in a spinning disk device (figure 1(A)), we derived the fluid flow and resulting forces theoretically and compared them to experimental data. First, we verify that our values for the variables *F*, *G* and *H* which are the local axial, azimuthal (tangential), and radial velocity components are in good agreement with literature values Schlichting [14] and Sohrab [16] (figure 1(B)). Given its cell detachment force application, we then calculated the flow field above the spinning disk with the following constraints: a 5400 rpm rotation speed, $0.7 \times 10^{-6}\ m^2\ s^{-1}$ viscosity, and a 25 mm coverslip diameter. Due to the no-slip condition, all fluid velocity components at the coverslip were zero as expected. Close to the surface where cells are (<10 μm), vertical velocity, v_z, was negligible (<1 mm s^{-1}) compared to radial, v_r, and azimuthal, v_θ, velocities (figure 1(C)). For these conditions, the components of the shear stress on the disk surface were 834 (azimuthal, τ_θ) and 661 dyne/cm^2 (radial, τ_r); thus the total shear stress was 1064 dyne/cm^2 applied at 38.4° from the azimuthal/tangential direction, independent of radial distance or angular velocity. The total shear stress was in excellent agreement compared to the previously published shear stress equation for spinning disk assays [18, 19]:

$$\tau = \frac{4}{5} r \sqrt{\rho \mu \omega^3}, \qquad (1)$$

where *r* denotes radial distance, ρ the fluid density, μ the dynamic viscosity, ω the rotational velocity and which yields a theoretical shear stress of 1079 dyne/cm^2. Rounding the pre-factor to 4/5 which is commonly done causes the negligible increase in shear force.

To verify that the shear forces were correctly estimated by equation (1) and that detachment is a function of applied shear, we modulated the kinematic density η ($\eta = \mu \times \rho$) and the angular velocity ω to determine assay sensitivity. This was done in high cation concentrations containing $CaCl_2$, where cells exhibit classical sigmoidal detachment characteristics [5, 10]. Using equation (1) to transform radial positions into shear stress, cell density as a function of shear stress was plotted for a range of angular velocities (figure 2(A)). Data from all velocities overlapped and

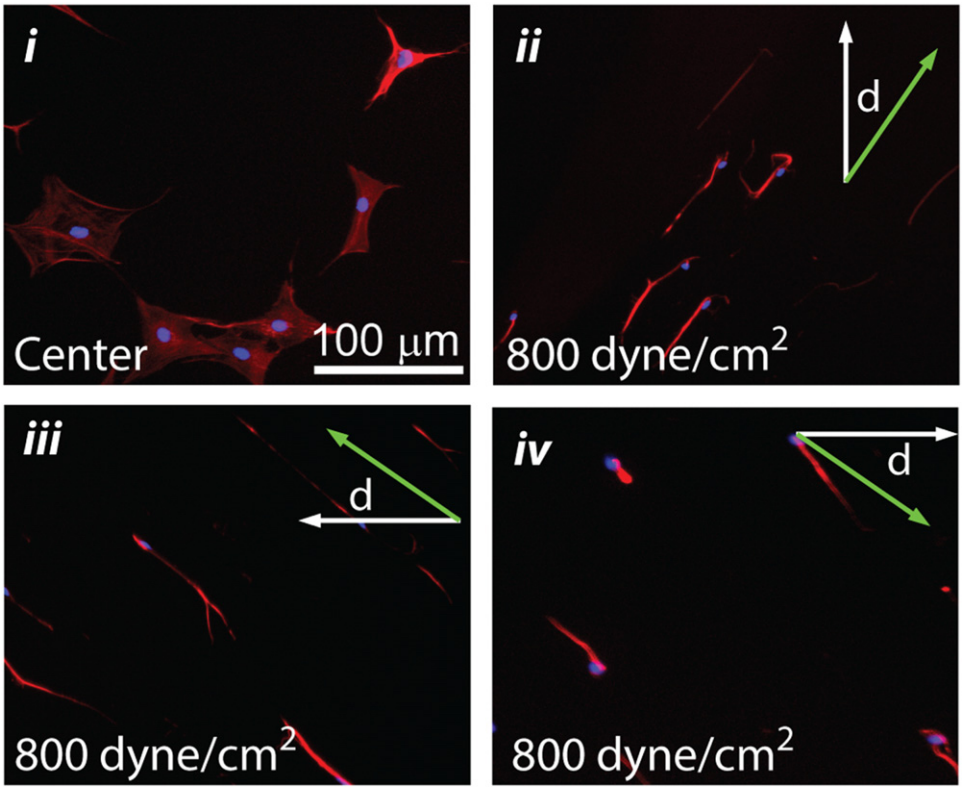

Figure 4. Cell alignment with acute shear. Fluorescent images of cells at different positions on the coverslip after application of shear as indicated (blue = dapi, red = actin). The direction of shear is indicated by the green arrows and the azimuthal direction by the white arrows. Rotational speed 5400 rpm ($\tau = 800$ dyne/cm^2; $r = 8$ mm). Same scale for all for images.

could be well fitted by a single sigmoidal curve. Attachment strength also appeared independent of viscosity (η) modification (a seven-fold increase) when comparing equivalent shear (figure 2(B)). Note that fibrosarcoma cells were used with viscosity modification due to their insensitivity to glycerol treatment (see Materials and Methods). While these data validate that rotational speed, radial position, and viscosity are correctly considered in equation (1), the pre-factor of 4/5 remains to be verified.

Unlike with conventional buffers containing $CaCl_2$, we recently observed that fibroblast detachment can be dominated by cytoskeletal remodeling in $CaCl_2$-free but $MgCl_2$-containing buffer conditions [5]. Here we find that seeding cells without serum increased remodeling efficiency. ~60% of cells seeded without serum for 24 h detached at a shear stress in excess of 600 dyne/cm^2 while the remaining 40% withstood shear stress up to 1000 dyne/cm^2 and were markedly elongated in shape (figure 3). At 800 dyne/cm^2 and at the indicated radial and azimuthal positions, the alignment of cells visually coincided with shear direction (figure 4, green arrow). Subsequent quantification of cell alignment shows that cells indeed undergo morphological change and are tightly aligned at higher shear (figure 5(A)). With sufficient shear, local cell alignment throughout the coverslip (figure 5(B), red arrows) was close to the predicted direction (inset, black arrows). Note that cell alignment with shear stress direction, i.e. the angle d, was independent of azimuthal position but dependent on radial position as shown in figures 4 and 5.

To establish that alignment was due only to the shear force magnitude (figure 1) and direction (figure 5), coverslips were spun at multiple angular velocities. Cells gradually align with increasing shear and reach full alignment at shear above 600 dyne/cm^2 (figure 6(A)) and fibroblast alignment occurred independent of angular velocity (figure 6(A)). Alignment was also independent of acute shear exposure time (figure 6(B)) with alignment occurring close to the predicted direction of shear in all cases and when data is combined (dashed line in figure 6(B)). Small variations in these data likely represent systematic error such as coverslip placement.

The forces on the cells are morphology-dependent, e.g. for semi-spherical cells drag and torque dominate [20]. However, given sufficient time, most cells fully spread on a substrate with only the nucleus experiencing significant force from drag and torque. Furthermore, in standard cation conditions (i.e. with $CaCl_2$) cells do not align [5]. Cells under shear can then be adequately modeled as a section of a sphere with its maximum height (figure S1), a geometry which has been previously solved numerically [21]. We estimate the forces that act on the cells in the appendix which can be found in the supplementary information stacks.iop.org/PB/12/016011/mmedia. While we do this with the

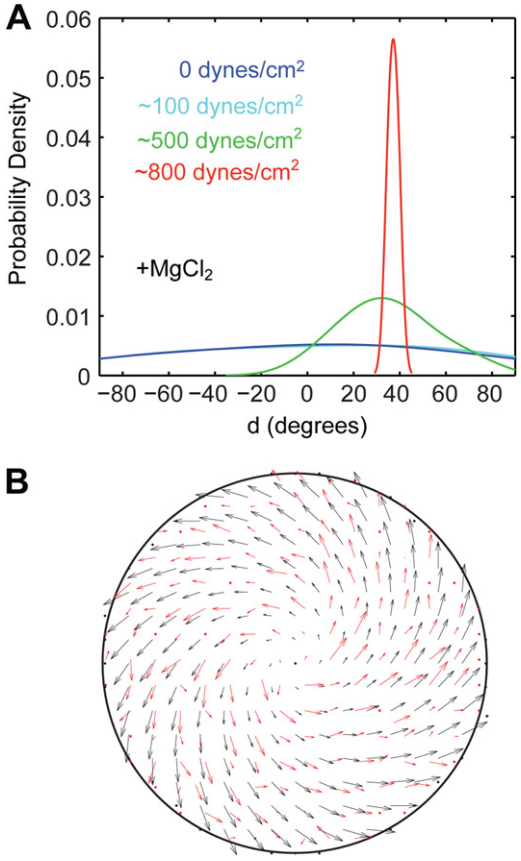

Figure 5. Quantification of alignment with acute shear. (A) Probability density (frequency) of the cell orientation angle d at radial distances corresponding to the indicated shear forces. (B) Shear orientation (black) compared to average cellular orientation (red). All data are shown for $z = 0$.

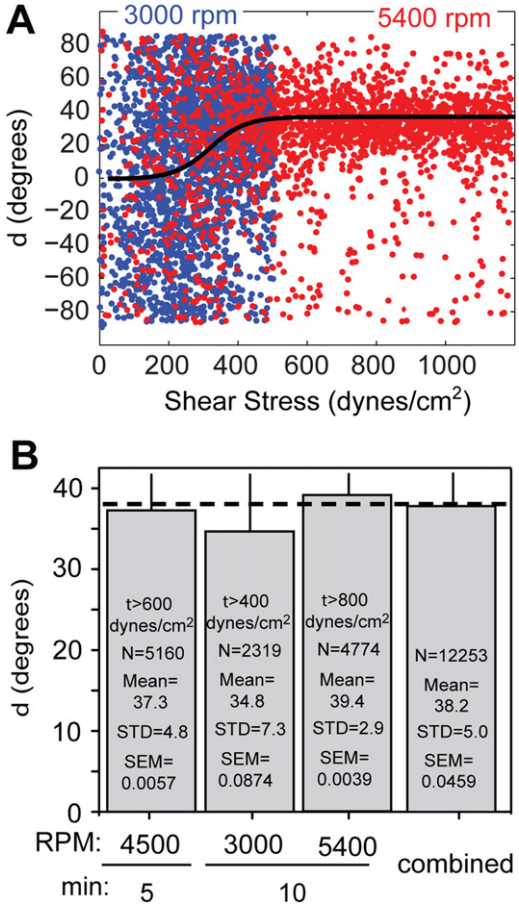

Figure 6. Verification of shear flow direction. (A) Cell angle from azimuthal versus shear stress. For better visibility only every 5th data point is plotted. (B) Cell angle from azimuthal plotted for indicated angular velocities and exposure times. Dashed line represents theoretical value.

parameters of the cell type used here, this can also be used as a guideline for different parameters, such as cell type. In brief, we find that for the 3T3 fibroblasts used here differences in drag and torque forces resulting from variations in morphology are negligible compared to force due to the wall shear stress. Attachment strength as function of shear force per cell area can therefore be directly assessed without further modeling. However, as the limits of this assumption depend on specific parameters, they need to be verified when studying different conditions, e.g. cell types, ligands or adhesion times.

Conclusions

These data (1) demonstrate that cells align in the direction of applied shear within minutes under calcium free conditions and (2) verify the shear flow direction and magnitude (equation (1)). We previously found that cell alignment under acute shear involves $\alpha_5\beta_1$ integrin and that aligned cells remain viable [5]. It is important to note that this a morphological adaptation rather than a selection of cells with that specific morphology. However, the detailed mechanisms by which this alignment takes place and the mechanism by which alignment efficiency is improved when cells are serum-starved remain undetermined. The effects and mechanisms of the acute shear seen here, which is intended to load existing cell-matrix adhesions and not induce long-term remodeling, are also likely different from cell behavior due to chronic shear. We speculate that alignment allows the cell to reduce the sum effective force it experiences under flow, allowing them withstand detachment despite increasing shear (figure 4; note the plateau of cell density between 600 and 1000 dyne/cm^2). Nevertheless, it is evident that this drastic morphological adaptation affects apparent attachment strength and therefore needs to be carefully monitored when assessing adhesion by shear assays. In calcium containing media without cell alignment, we completed verification of the shear flow equation (equation (1)). In turn this also demonstrated that cell detachment is indeed a function of the applied force. This allowed us to show that attachment strengths of different spread cell types or different cellular treatments can be directly compared. Forces would only need to be normalized to cell spread area in case total applied force as opposed to force applied per area is of interest. Together our data

strengthen the applicability and reliability of the spinning disk method but also other shear flow devices for the quantitative investigation of cell–matrix interactions.

Acknowledgments

The authors thank Juan Carlos del Alamo and Gaurav Kaushik for helpful discussions of fluid mechanics and proofreading. The authors acknowledge the National Institutes of Health (U54CA143803-03 and DP02OD006460) for funding.

References

[1] Berrier A and Yamada K 2007 Cell–matrix adhesion *J. Cell. Physiol.* **213** 565–73
[2] Katsumi A, Orr A W, Tzima E and Schwartz M A 2004 Integrins in mechanotransduction *J. Biol. Chem.* **279** 12001
[3] Engler A J, Sen S, Sweeney H L and Discher D E 2006 Matrix elasticity directs stem cell lineage specification *Cell* **126** 677–89
[4] Plotnikov S V, Pasapera A M, Sabass B and Waterman C M 2012 Force fluctuations within focal adhesions mediate ECM-rigidity sensing to guide directed cell migration *Cell* **151** 1513–27
[5] Fuhrmann A, Li J, Chien S and Engler A J 2014 Cation type specific cell remodeling regulates attachment strength *PLoS One* **9** e102424
[6] Kumar S and Weaver V M 2009 Mechanics, malignancy, and metastasis: the force journey of a tumor cell *Cancer Metastasis Rev.* **28** 113–27
[7] Friedrichs J *et al* 2013 A practical guide to quantify cell adhesion using single-cell force spectroscopy *Methods* **60** 169–78
[8] Garcia A J and Gallant N D 2003 Stick and grip: measurement systems and quantitative analyses of integrin-mediated cell adhesion strength *Cell Biochem. Biophys.* **39** 61–73
[9] Marshall B T *et al* 2003 Direct observation of catch bonds involving cell-adhesion molecules *Nature* **423** 190–3
[10] Boettiger D 2007 Quantitative measurements of integrin-mediated adhesion to extracellular matrix *Methods Enzymol.* **426** 1–25
[11] Tzima E *et al* 2002 Activation of Rac1 by shear stress in endothelial cells mediates both cytoskeletal reorganization and effects on gene expression *EMBO J.* **21** 6791–800
[12] Cheng N 2008 Formula for the viscosity of a glycerol-water mixture *Ind. Eng. Chem. Res.* **47** 3285–8
[13] Kármán T V 1921 Über laminare und turbulente reibung *ZAMM—J. Appl. Math. Mech. Angew Math. Mech.* **1** 233–52
[14] Schlichting H 1968 *Boundary-Layer Theory* 539th edn (New York: McGraw-Hill)
[15] Cochran W G 1934 The flow due to a rotating disk *Proc. Camb. Phil. Soc.* **30** 365–75
[16] Sohrab S 2005 A modified theory of laminar flow near a rotating disk *IASME Trans.* **1** 152–9
[17] Berens P 2009 Circstat: a MATLAB toolbox for circular statistics *J. Stat. Softw.* **31**
[18] Horbett T A, Waldburger J J, Ratner B D and Hoffman A S 1988 Cell adhesion to a series of hydrophilic–hydrophobic copolymers studied with a spinning disc apparatus *J. Biomed. Mater. Res.* **22** 383–404
[19] García A J, Ducheyne P and Boettiger D 1997 Quantification of cell adhesion using a spinning disc device and application to surface-reactive materials *Biomaterials* **18** 1091–8
[20] Gallant N D and García A J 2007 Model of integrin-mediated cell adhesion strengthening *J. Biomech.* **40** 1301–9
[21] Pozrikidis C 1997 Shear flow over a protuberance on a plane wall *J. Eng. Math.* **31** 29–42